

RETROFIT OF PRE-NORTHRIDGE MOMENT-RESISTING CONNECTIONS

By Scott A. Civjan,¹ P.E., Michael D. Engelhardt,² P.E.,
and John L. Gross,³ P.E., Members, ASCE

ABSTRACT: An experimental program was undertaken to evaluate methods to retrofit existing steel moment connections for improved seismic performance. Six full-scale subassemblages were tested under cyclic loading. Typical pre-Northridge connections were retrofit by the addition of either a bottom flange dogbone or a welded bottom flange haunch. Retrofitted specimens were tested both with and without a composite floor slab. The tests showed poor performance of the bottom flange dogbone retrofit when the existing low toughness welds were left in place. Somewhat improved performance was observed when the bottom flange dogbone was combined with replacement of beam flange groove welds with higher toughness welds. The welded bottom haunch retrofit showed excellent performance on specimens with a composite slab, even though the existing low toughness beam flange groove welds were left in place. The presence of the composite slab appeared to help prevent fracture of the existing top flange weld in the haunch retrofit. This paper provides a summary of the complete experimental program.

INTRODUCTION

Damage to steel moment resisting frames (SMRFs) due to the 1994 Northridge California earthquake was extensive, indicating that the typical SMRF welded flange-bolted web connection detail used from the early 1970s had inherent performance problems. The implications of this damage are far reaching, as the connection detail was used throughout California and other seismically active areas for over twenty years.

After the Northridge earthquake, damage reports indicated that prevalence of bottom flange weld fractures in the absence of inelastic beam deformations (Youssef et al. 1995). Major factors contributing to observed damage include the low fracture toughness of pre-Northridge connection welds, the stress concentrations and general flange overstress present in the typical connection, the influence of leaving steel backing bars in place (leading to stress concentrations, possible weld inclusions, and added difficulty inspecting the welds), the stop-and-start bottom flange weld procedure, and the presence of a composite slab (*Proceedings* 1994; Yang and Popov 1995; Miller 1996; Sabol and Engelhardt 1996; Kaufmann et al. 1997; Ojdrovic and Zarghamee 1997).

Post-Northridge testing of pre-Northridge connection details corroborated the damage observed in the Northridge earthquake (Engelhardt and Sabol 1994; Yang and Popov 1995; Shuey and Engelhardt 1996; Uang and Bondad 1996). Successful solutions for new construction design have been tested, including flange cover plate, ribbed connection, haunch, dogbone designs and many others (Engelhardt and Sabol 1994; Plumier 1995; Uang and Noel 1995; Chen et al. 1996; Engelhardt et al. 1996; Iwankiw and Carter 1996; Shuey and Engelhardt 1996; Uang and Bondad 1996; Tremblay et al. 1997; Xue et al. 1997). These improved connections utilized higher toughness electrodes and other weld improvements, in addition to design modifications.

Relatively little testing has studied effects of a composite slab on steel moment connection behavior under cyclic loads.

Most testing of composite specimens to date has included a fully composite slab with significant amounts of slab reinforcement. When subjected to cycled positive moments, the slab contribution under positive moment has been determined as a compression zone emanating from the face of the column flange. The compressive stress acting at this location was reported as $1.3f'_c$ (Du Plessis and Daniels 1972), although a specimen subjected to reversed cyclic loads did not reach the estimated moment capacity based on this assumption (Lee and Lu 1989). Reversed cyclic testing of a full frame indicated a compressive stress at the column face of $1.8f'_c$ (Tagawa et al. 1989). These previously tested specimens were fully composite with respect to gravity load conditions. A bare steel and two "partially" composite specimens were tested by Leon et al. (1998). Bottom weld failures occurred in all three specimens.

Previous connection testing has concentrated on pre-Northridge connections, new construction designs, and repair methods. Less testing has been directed towards retrofit methods for existing moment connections. In addition, the presence and influence of a concrete slab is not fully understood for the case of a laterally loaded structure. This project was therefore undertaken to investigate the effects of relatively inexpensive and nonintrusive retrofit procedures on connection performance. The influence of a building slab on the connection retrofit was also studied. Additional information on the project can be found in Civjan (1998).

This testing program was part of a larger research program on retrofit of existing steel moment connections coordinated by the National Institute of Standards and Technology. Details of the complete program can be found in Gross et al. (1999). As part of this larger coordinated program, additional tests on dogbone and haunch retrofit techniques were also conducted at the University of California at San Diego, as reported by Uang et al. (1998).

EXPERIMENTAL TEST SETUP AND SPECIMENS

Tests were performed on full-sized interior joint subassemblages. Points of inflection were assumed at column story midheights and at beam midspans. A typical story height and beam span were assumed. The overall test frame schematics can be seen in Fig. 1.

The test specimens were chosen to be representative of building construction details in common use prior to the Northridge Earthquake and not to duplicate specimens investigated elsewhere. Beams were W30 × 99 sections of A36 steel. Columns were W12 × 279 sections of A572 Grade 50 steel to provide strong column, weak beam action and to pro-

¹Asst. Prof., Univ. of Massachusetts at Amherst, Dept. of Civ. and Envir. Engrg., 139 Marston Hall, Box 35205, Amherst, MA 01003-5205.

²Assoc. Prof., Univ. of Texas at Austin, Dept. of Civ. Engrg., Phil M. Ferguson Engrg. Lab., 10100 Burnet Rd., Bldg. 177, Austin, TX 78758.

³Nat. Inst. of Standards and Technol., Struct. Div., 100 Bureau Dr., Stop 8611, Gaithersburg, MD 20899-8611.

Note. Associate Editor: Brad Cross. Discussion open until September 1, 2000. To extend the closing date one month, a written request must be filed with the ASCE Manager of Journals. The manuscript for this paper was submitted for review and possible publication on July 1, 1999. This paper is part of the *Journal of Structural Engineering*, Vol. 126, No. 4, April, 2000. ©ASCE, ISSN 0733-9445/00/0004-0445-0452/\$8.00 + \$.50 per page. Paper No. 21298.

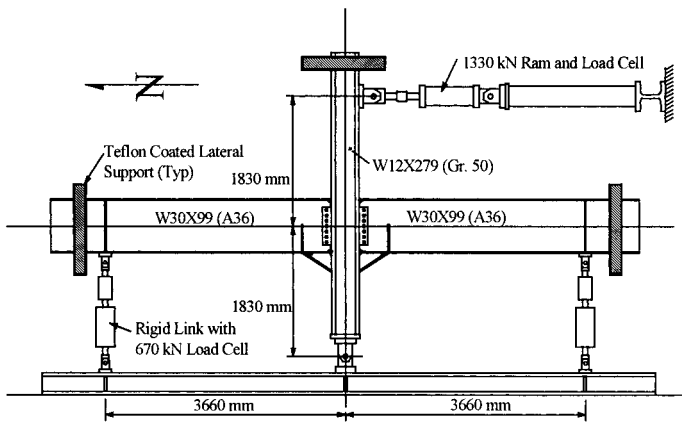


FIG. 1. Test Frame Schematic

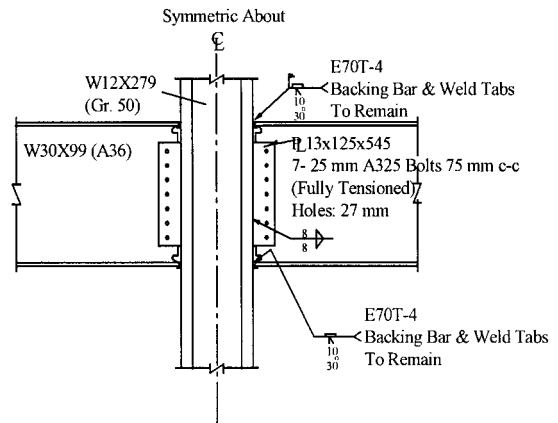


FIG. 2. "Original" Connection Details

vide for a strong panel zone. Three pairs of specimens were tested. Each pair consisted of a bare steel specimen and a similar specimen with a composite slab attached. In the first pair, the dogbone retrofit was investigated. In the second and third sets, a haunch retrofit with slightly differing weld procedures was investigated. In keeping with the actual construction sequence, the specimens were assembled as an "original connection" and then retrofitted. Specimens of pre-Northridge design with $W30 \times 90$ beams were tested previously as part of the SAC program (FEMA 1997a). These previous results were referenced as a benchmark for the performance of the retrofit specimens. Overall specimen details are compiled in Table 1. Beam materials came from four separate heats of steel with average measured stresses of: static yield 329 MPa (47.7 ksi), dynamic yield 345 MPa (50.0 ksi) and dynamic ultimate 452 MPa (65.6 ksi).

The "original" connection was designed, detailed, and constructed in a manner typical of mid-1970s pre-Northridge building construction. Past editions of the Uniform Building Code (UBC), structural engineers, fabricators, and erectors were consulted regarding past design and construction practice. Details of the connection are shown in Fig. 2. The test specimens are not representative of cases with weak column panel zones, as were permitted by the 1988 UBC code. The 1988 UBC code required supplemental web welds for the test specimens which were not provided. It was believed that a larger number of existing moment frame buildings were designed prior to the 1988 UBC and therefore would not likely have included these additional welds.

The dogbone retrofit method required some special considerations. First, discussions with fabricators indicated that cutting a dogbone in the beam top flange in the presence of a floor slab would likely be difficult and costly. Consequently, a dogbone cutout was provided in the bottom flange only. Second, the flange area reduction was limited to a maximum of

50% of the total flange area due to concerns over the stability of the beam should larger reductions be provided. The tested dogbone cutout permitted substantially less moment reduction at the face of the column compared with typical dogbone connections tested for new construction applications, where cutouts are provided in both flanges. Dogbone details including weld improvements can be seen in Fig. 3.

After fabrication of the "original" connection, the dogbone contours were manually torch cut and ground smooth in a direction parallel to the flange. Additional weld improvements were made in the composite dogbone specimen (DB2) in response to poor performance of the bare steel specimen's bottom weld.

The haunch retrofit consisted of welding a wide flange section into the area of intersection of the bottom beam flange and column flange. A pair of stiffeners was also placed at the end of the haunch to distribute the vertical forces into the beam web. Details of the haunch retrofit can be seen in Fig. 4. Bare steel specimens (HCH1 and HCH3) and composite specimens (HCH2 and HCH4) were tested. Sizing of the haunch was chosen to replicate details tested by Uang and Bondad (1996).

One of each pair of similar specimens included a 2,440 mm (8 ft) wide composite slab. The goal was to observe the effects of a typical building slab on composite connection performance. Detailing was representative of past construction practice in California and was recommended by practicing engineers. Metal decking was oriented perpendicular to the beams and lightweight concrete was used. The number and location of shear studs was chosen to be representative of existing buildings. These shear studs do not provide fully composite action as defined by the AISC LRFD code. They do, however, provide the capacity of the expected maximum compressive force in the concrete slab, estimated to be $1.3f_c$ times the effective slab area in contact with the column flange, as per Du Plessis and Daniels (1972). Studs were hand fillet welded to

TABLE 1. Specimen Details

Specimen (1)	Type of retrofit (2)	Modification to Beam Flange Welds		Composite or bare steel (5)
		Top flange (3)	Bottom flange (4)	
DB1	Bottom flange dogbone	None	Backing bar and weld tabs removed	Bare steel
DB2	Bottom flange dogbone	E70T-4 completely removed reweld with E71T-8 weld tabs removed, backing bar left in place with seal weld to column	E70T-4 completely removed reweld with E71T-8 backing bar and weld tabs removed	Composite
HCH1	Bottom haunch	None, flaws left in place in north & south beams	None, flaws left in place in south beam	Bare steel
HCH2	Bottom haunch	None, flaws left in place in north & south beams	None, flaws left in place in south beam	Composite
HCH3	Bottom haunch	None	None, flaws left in place in north and south beams	Bare steel
HCH4	Bottom haunch	Weld tabs inadvertently removed	None, flaws left in place in north beam	Composite

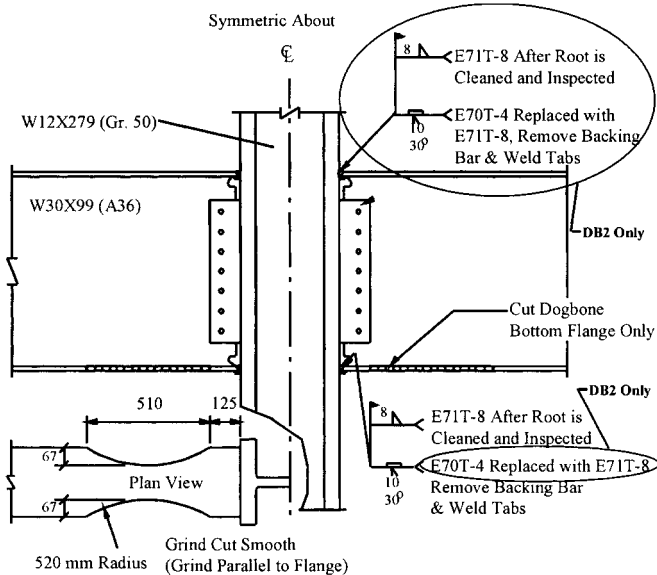


FIG. 3. Dogbone Retrofit Details

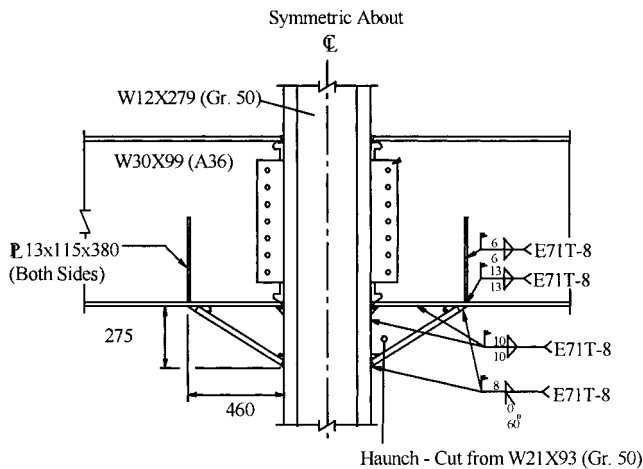


FIG. 4. Haunch Retrofit Details

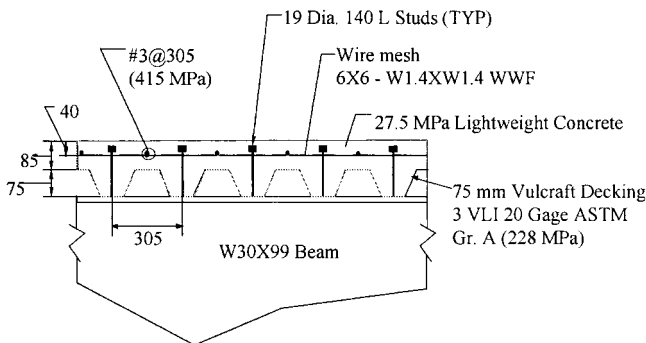


FIG. 5. Slab Details—Section View

the beam flange using SMAW with E7018 electrodes. Number three reinforcing bars were placed perpendicular to the beams to prevent longitudinal temperature and shrinkage cracking and 6 × 6 welded wire mesh was installed. This wire mesh provided the only longitudinal reinforcement in the slab, with the exception of two number three bars running along the perimeter of the slab. The number three bars were added to maintain a realistic boundary condition at the slab edges. Details of the slab are shown in Fig. 5. Concrete compressive strengths on the day of testing were 33.7, 42.3, and 22.2 MPa

(4,883, 6,132, and 3,220 psi) for specimens DB2, HCH2, and HCH4, respectively.

Welds in the “original” connection were made using the self-shielded flux core arc welding (SS-FCAW) process with a 3 mm (0.120 in.) diameter E70T-4 electrode. Backing bars and weld tabs were left in place for the “original” connection. All “retrofit” welds were made using SS-FCAW with a 1.8 mm (0.072 in.) E71T-8 electrode. All welding was performed in accordance with AWS D.1.1-94. Measured weld Charpy V-notch values averaged 18.6 N-m (13.7 ft-lb) (21.1°C) and 6.4 N-m (4.7 ft-lb) (−28.9°C) for the E70T-4 electrode and 94.9 N-m (70.0 ft-lb) (21°C) and 45.7 N-m (33.7 ft-lb) (−28.9°C) for the E71T-8 electrode.

All welds were ultrasonically tested by a commercial weld inspection firm with acceptance criteria based on table 8.2 of AWS D1.1-94. “Original connection” welds were left “as is.” The exception to this was the final set of haunches (specimens HCH3 and HCH4), in which “original connection” top flange welds were repaired until they passed inspection. Rejectable defects remained in the bottom flanges of HCH1, HCH2, HCH3, and one side of HCH4, as well as one top weld in both HCH1 and HCH2. “Retrofit” welds were tested when they were critical.

EXPERIMENTAL RESULTS

For the purposes of this study, the overall performance of the retrofitted specimens was judged by total plastic rotation. An acceptance criterion of 0.020 radian total plastic rotation for retrofitted connections is recommended by Gross et al. (1999). This criterion would provide a significant improvement in performance as compared with existing pre-Northridge connections. Note that this is lower than the 0.030 radian recommended by the “Interim Guidelines” (FEMA 1995) and “Advisory No. 1” (FEMA 1997b) for new construction.

Loading History

The specimens were loaded under quasi-static cyclic loading as per ATC-24 (ATC-24 1992) guidelines. The load history is based on δ_y , the estimated yield displacement of the specimen. In order to be able to directly compare all the results, load histories are based on the δ_y of the “original” connection, which corresponded to a column tip displacement of 30 mm (1.2 in.).

Overall Specimen Performance

The load versus column tip deflection (δ_{tot}) as well as the story drift is plotted for several specimens in Fig. 6. Photographs of selected specimens after testing are shown in Fig. 7. Specimens HCH1 and HCH2 results were very similar to HCH3 and HCH4, respectively. A summary of the test results is presented in Table 2. These results can be compared with a previous testing of W30 × 99 beams of pre-Northridge connection details that was performed as part of the SAC initiative and compiled previously (FEMA 1997a). In these previous tests, E70T-4 electrodes were utilized. However, there were several differences from the specimens in this project. First, supplemental shear tab welds and continuity plates were used [each of which may improve connection performance (Popov et al. 1986; Tsai et al. 1994)]. Also, columns were of W14 × 176 shapes. The connections tested were only one sided, yet this smaller column shape allowed for panel zone plastic rotations on the order of the beam plastic rotations. The specimens tested as part of this project were dominated by beam plastic deformations. Panel zone deformations have been shown to increase total plastic rotations (Tsai et al. 1994). Each of the six similar previously tested specimens (FEMA 1997a)

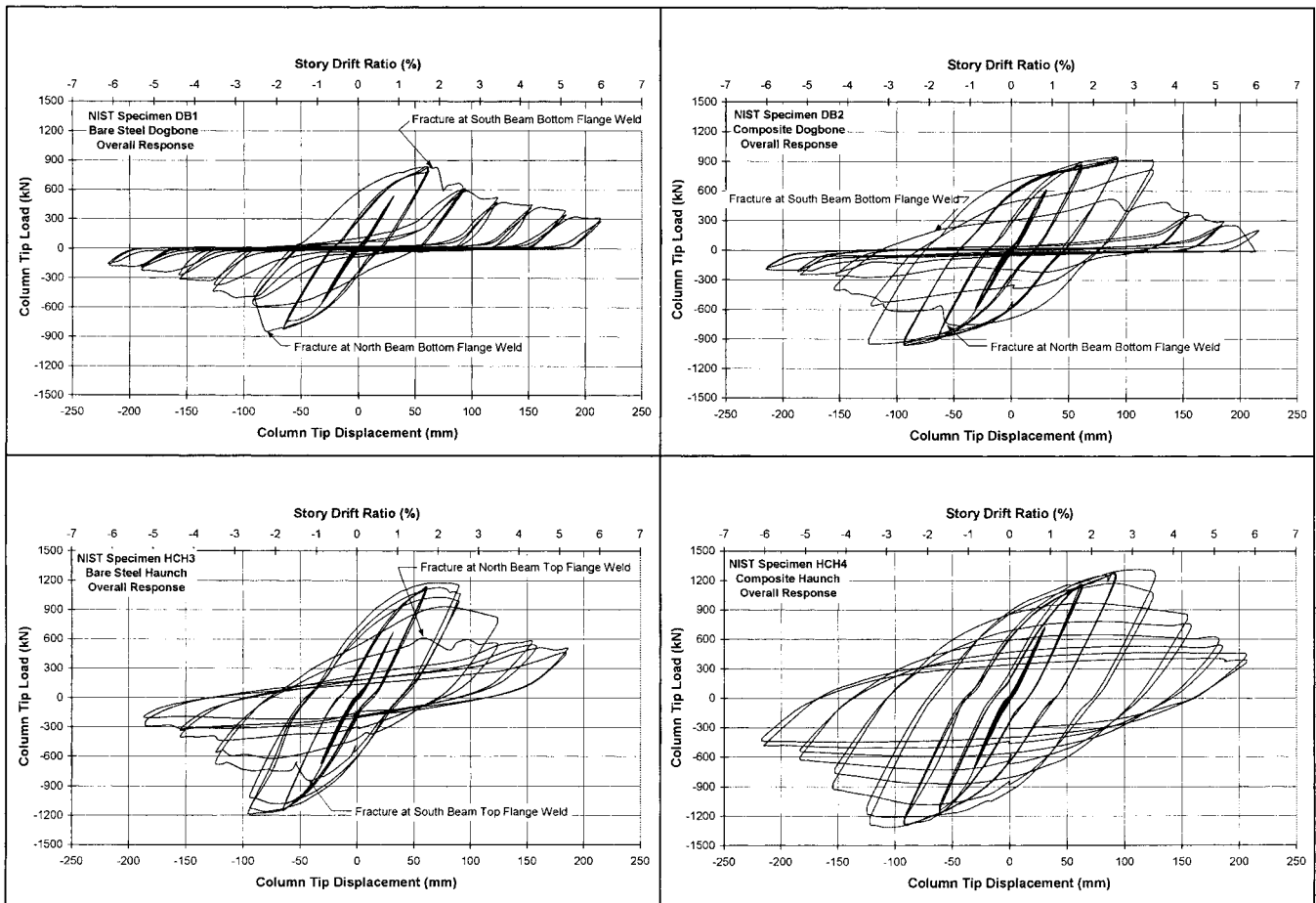


FIG. 6. Specimen Load versus Story Drift/Tip Deflection

resulted in fractures of the beam flange weld or the heat-affected zone. These fractures occurred at total plastic rotations of 0.008–0.021 radian. Approximately half of these rotation values were associated with beam deformations.

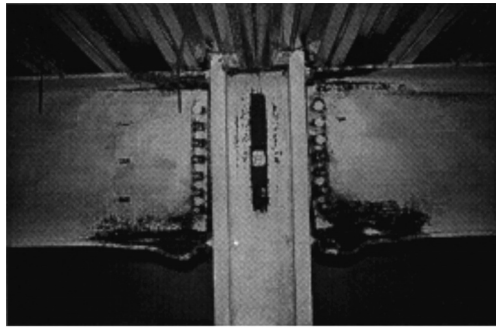
The bare steel bottom flange dogbone (DB1) exhibited the poorest performance of all specimens tested. Bottom flange groove welds for both beams failed within the existing low toughness weld metal, near the weld-beam interface, at low levels of total plastic rotation (0.006 and 0.009 radian). The fractures appeared to initiate at the center of the flange, near the beam web cope. This specimen did not provide any increase in performance over a nonretrofitted connection.

The composite bottom flange dogbone (DB2) exhibited a marked improvement over specimen DB1, achieving beam plastic rotations of 0.020 radian. Both connections, however, still failed by fracture of the bottom flange groove welds. During the 120 mm (4.80 in.) load cycles, fractures initiated at the bottom cope holes and propagated along the bottom edge of the beam web with each cycle. This was followed during the next cycle at 120 mm (4.80 in.) by the fracture of the bottom flange groove weld in both beams. The fractures initiated at the center of the beam flanges, near the beam web cope. Inspection of the weld fracture surfaces revealed some rather large slag inclusions not detected by ultrasonic testing, which may have contributed to the weld failures. Specimen DB2 sustained much higher levels of plastic rotation than DB1, likely due to a substantial benefit from the higher toughness weld metal (composite slab effects were also involved.) Once the bottom flange welds of DB2 failed, the behavior was extremely poor and degraded substantially during later load cycles. Although the specimen obtained beam plastic rotations meeting or exceeding the 0.020 radian of plastic rotation ac-

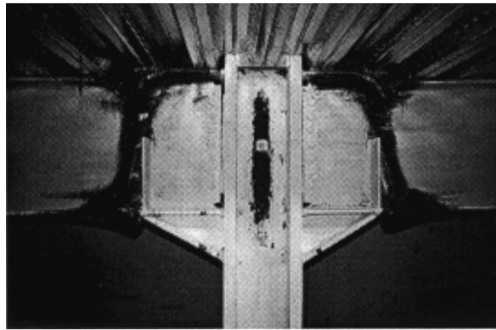
ceptance criteria, the weld fractures occurred at levels very close to this acceptance criteria. Variations in slab details, such as stronger concrete, more reinforcing steel, or steel decking oriented in the other direction, may cause earlier fractures. Therefore, the connection detail tested must be viewed with caution.

Three of the four bare steel bottom haunch connections (specimens HCH1 and HCH3) failed by fracture of the existing E70T-4 top flange welds at total plastic rotations in the range of 0.012–0.023 radian. The similar behavior of specimen HCH3 confirmed that that the haunch retrofit is vulnerable to fracture at the existing low toughness top flange weld, even when precautions are taken to ensure that the existing weld contains no rejectable defects. The fractures appeared to initiate at the edge of the beam flanges. Little deterioration in the overall strength of the specimen was observed until the fracture propagated across the full flange width. Significant local buckling and lateral torsional buckling of the beams as well as some twisting of the column was observed in the latter cycles of the test. After weld fracture, the haunch specimens (HCH1 and HCH3) showed a significantly higher residual strength than the dogbone specimen (DB1). The fourth connection (south beam of HCH1) did not fail by fracture, but simply deteriorated gradually due to local and lateral buckling. These specimens performed better than DB1, although the bottom haunch retrofit may still be vulnerable to fracture at the existing low toughness top flange welds. These results suggest that, if existing welds are not replaced with higher toughness weld metal as part of a connection retrofit, then the haunch may provide a greater improvement in connection performance as compared with the bottom flange dogbone.

With the addition of a composite floor slab (specimens



(a)



(b)

FIG. 7. Photograph of Specimens after Testing: (a) DB2 after Testing; (b) HCH4 after Testing

HCH2 and HCH4) the connection behavior was excellent. All four connection beam flexural capacities deteriorated gradually due to local and lateral buckling of the beams. The top weld fractures of specimens HCH1 and HCH3 were prevented. Testing of both specimens was stopped due to testing limitations, with total plastic rotations of 0.028–0.055 radians.

Peak rotations were often associated with a substantial loss of load-carrying capacity. All connections (with the exception of the north beam of HCH3) that achieved 0.20 radian of total plastic rotation sustained in excess of 80% of the peak attained moment when reaching this critical rotation.

Test Specimen Forces and Strength

Estimated plastic moment capacities of the W30 × 99 beam sections were calculated at two locations for each specimen: at the column face and at the critical section. The critical section is defined as the center of the dogbone reduction or the end of the haunch. Calculated values are presented in Table 3. Estimated capacities were 25–35% higher than nominal capacities for the bare steel sections (10–35% for composite), primarily due to overstrength of the delivered steel. Estimated

TABLE 3. Estimated Plastic Moment Capacities

Specimen (1)	At Face of Column M_e (kN-m)		At Critical Section M_{ecr} (kN-m)	
	$M-$ (2)	$M+$ (3)	$M-$ (4)	$M+$ (5)
DB1	1,680	1,680	1,400	1,400
DB2	1,680	2,190	1,400	1,820
HCH1	2,870	2,870	1,670	1,670
HCH2	2,870	4,020 (3,650)	1,670	2,290 (2,100)
HCH3	2,950	2,950	1,730	1,730
HCH4	2,910	3,530 (3,330)	1,710	2,060 (1,940)

Note: Composite values based on $1.3f_c$ slab compressive stress over column face. Numbers in parenthesis correspond to value of $0.85f_c$ slab compressive stress acting over column face. Critical section is center of dogbone or end of haunch location.

capacities were based on the actual measured section dimensions, the dynamic tensile yield coupon data of the web and flanges, and concrete compressive strengths on the day of testing. Assumptions of concrete effective width equal to the column flange width and maximum compressive strengths of $1.3f_c$ were used [as recommended by Du Plessis and Daniels (1972)]. Only concrete above the metal decking flutes was considered effective and the minimal longitudinal reinforcement was neglected. Slab contributions in tension and strain hardening were neglected in these calculations.

Table 4 reports maximum attained values of bending moment for all tested specimens as a percentage of estimated plastic moment capacities. Results are reported at the face of the column and the critical section (center of dogbone cutout, end of haunch).

As expected, dogbone specimens did not reach the estimated plastic capacities at the column face in any specimen. At the critical sections both the bare steel and composite specimen only achieved the estimated plastic capacity in negative bending of one beam.

The attained capacities of the composite haunch specimens exceeded estimated values for the negative moment at the end of the haunch location. These ratios are generally larger than the bare steel ratios, indicating that there was some tensile capacity being contributed by the slab. This occurred even after a large crack had opened across the entire slab at the column face. Composite haunch attained capacities were generally lower than calculated values for the positive moment. This could either indicate that the assumption of $1.3f_c$ was an overly optimistic assumption for the compressive slab stresses, or that the shear and failures (discussed later) occurred before the maximum moments could be attained.

An additional comparison of estimated composite haunch plastic moment capacities is shown in parenthesis in Table 4. Here, an assumption of $0.85f_c$ is used for the maximum compression in the concrete (rather than the $1.3f_c$). Concrete ef-

TABLE 2. Test Results

Specimen (1)	Brief Description of Failure		Total Plastic Rotation ^a	
	North beam (2)	South beam (3)	North beam (4)	South beam (5)
DB1	Fracture of bottom flange weld	Fracture of bottom flange weld	0.009 radian	0.006 radian
DB2	Fracture of bottom flange weld	Fracture of bottom flange weld	0.020 radian	0.020 radian
HCH1	Fracture of top flange weld	Gradual deterioration in strength due to local and lateral buckling	0.012 radian	0.044 radian
HCH2	Gradual deterioration in strength due to local and lateral buckling	Gradual deterioration in strength due to local and lateral buckling	0.030 radian	0.030 radian
HCH3	Fracture of top flange weld	Fracture of top flange weld	0.023 radian	0.013 radian
HCH4	Gradual deterioration in strength due to local and lateral buckling	Gradual deterioration in strength due to local and lateral buckling	0.050 radian	0.050 radian

^aTotal plastic rotation is computed with respect to centerline of column.

TABLE 4. Attained versus Estimated Plastic Moment Capacities

Specimen (1)	AT FACE OF COLUMN				AT CRITICAL SECTION			
	North Beam		South Beam		North Beam		South Beam	
	<i>M</i> − (2)	<i>M</i> + (3)	<i>M</i> − (4)	<i>M</i> + (5)	<i>M</i> − (6)	<i>M</i> + (7)	<i>M</i> − (8)	<i>M</i> + (9)
DB1	0.960	0.913	0.832	0.906	1.026	0.978	0.897	0.970
DB2	0.906	0.869	0.953	0.859	0.970	0.931	1.026	0.925
HCH1	0.737	0.740	0.697	0.721	1.096	1.103	1.035	1.076
HCH2	0.772	0.614 (0.678)	0.815	0.654 (0.721)	1.150	0.938 (1.022)	1.218	0.997 (1.086)
HCH3	0.704	0.704	0.704	0.712	1.047	1.047	1.047	1.054
HCH4	0.802	0.722 (0.766)	0.717	0.651 (0.692)	1.192	1.080 (1.145)	1.066	0.970 (1.029)

Note: Composite values based on $1.3f_c$ slab compressive stress over column face. Numbers in parenthesis correspond to value of $0.85f_c$ slab compressive stress acting over column face. Critical section is center of dogbone or end of haunch location.

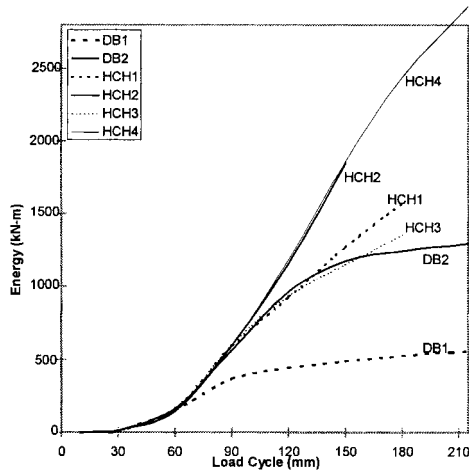


FIG. 8. Cumulative Dissipated Energy

fective width was still assumed equal to the column flange width. It can be seen that this assumption provides a lower bound of the compressive strengths (all positive moment ratios approach one). These modified ratios were similar to ratios observed for the bare steel specimens HCH1 and HCH3.

An overview of the cumulative energy dissipated by the specimens is shown in Fig. 8. The composite specimens showed a much greater capacity to dissipate energy than the corresponding bare steel specimens. At the end of the tests, all haunch specimens were still actively dissipating energy, while the dogbone specimens dissipated relatively little energy in later load cycles. Similar haunch specimens dissipated very similar amounts of energy at each load cycle, although the bare steel specimens diverged beyond the 120 mm (4.8 in.) load cycles, at which point specimen HCH1 had only one fractured weld while HCH3 had fractured welds in both beams.

Stud Failures

During the testing of the composite specimens, failure of shear studs at the welds often occurred. Locations of failed shear studs were determined through visual inspection. With the exception of the end shear studs, which spalled the end of the slab in all cases, all shear studs eventually failed in specimen HCH4, while in HCH2 only one stud near the column face was intact at the end of testing. Specimen DB2 did not reach the higher loads of the haunch specimens, and the shear studs were left mostly intact. All 24 shear studs in DB2 were still attached to the beam flange after demolition of the concrete slab, but five were easily removed by impacting the stud with a sledgehammer. Typically, shear stud welds severed, although at least one shear stud sheared completely through the stud itself. Although the specimens provided only partially composite action when gravity loading was considered, the

specimens were provided only partially composite action when gravity loading was considered, the specimens were provided with sufficient shear stud capacity to withstand a maximum concrete compressive force equal to $1.3f_c$ times the effective concrete area for lateral loads (width of column flange times slab thickness above the steel decking). This slab compressive force was not generally attained prior to the shear stud failures.

Failures of shear studs appeared to initiate in the 60 mm (2.4 in.) load cycles and continued through the 150 mm (6.0 in.) cycles. This loss of composite connection through the testing of the specimens made the slab influence at later cycles of loading much more difficult to evaluate. It was not possible to conclusively identify the cause of shear stud failures in the specimens. These stud failures may indicate an inadequacy in the shear stud strength provisions of the AISC specification when applied to cyclic loading, poor weld quality for the studs in the specimens, or additional forces on the studs due to twist of the specimens.

Slab Effects

The composite slab provided a slight increase in initial elastic stiffness and increased positive moment capacity 10–30% as compared with the base steel specimens. Negative moment capacities were often slightly increased by the composite slab, but this effect was not apparent in all specimens. Diagonal cracks propagating from both the column flange face and the inside edges of the far column flange were seen. It may therefore be speculated that maximum concrete compressive forces may not only be increased beyond f_c , but that the effective width of the compression zone at the column face is wider than the column flange.

A comparative measure of instability between bare steel and composite specimens could be inferred from examining beam shortening data. As local and lateral buckling of the beam occurs, the length of the beam in the specimen decreases. Shortening was measured over the full length of the beam (column face to the support). In comparing the beam shortening effects through the 90 mm (3.6 in.) load cycles, all of the bare steel specimens had divergent values for the east and west sides of the beam, indicating significant twist and distortion of the beam. Such behavior was still evident, but at a much smaller scale in the composite specimens. This disparity became even more extreme at later loading cycles. The large beam shortening values may indicate a deficiency in this type of testing at later load cycles.

Another significant effect of the slab on local instabilities can be seen in Fig. 9. The local buckling of the top flange for specimen HCH4 is shown at the 120 mm (4.80 in.) load cycle. It appeared that the top flange buckling was controlled by the slab and was significantly less severe than in the bare steel specimens. This, in part, may explain the absence of top flange weld failures in the composite specimens. The weld failures in both HCH1 and HCH3 appeared to initiate at the edge of



FIG. 9. HCH4 Buckled Shape of Top Flange [120 mm (4.8 in.) Load Cycle]

the beam flange in contrast to the dogbone weld fractures, which appeared to initiate at the center of the welds. It is possible that beyond the brittle fractures that occurred in Northridge and in specimen DB1, the next weld failure mode may be due to low cycle fatigue from high amplitude distortions associated with local buckling of the flange. The presence of a slab appeared to control this behavior very well at the top flange.

Additional Observations

Yielding patterns indicated that the distribution of stresses in the sections did not follow classical beam theory. For instance, the yielding of the specimens throughout testing showed bottom flange yielding at the critical section, but top flange yielding was concentrated at a location much closer to the column face (Fig. 7). This indicated an active cross section for inelastic action that was not oriented perpendicular to the beam's longitudinal axis.

Flange strains were decreased at the top flange when a composite slab was added, although strains at the bottom flange remained similar. It is often assumed that the presence of a slab will increase bottom flange strains. The increase in moment may be offset by the increased section depth, resulting in little change to bottom flange strains. This will be discussed in more detail in a separate paper. Strains were much more uniform across the flange width at the critical section than at the column face. Early yielding indicated high residual stresses at the column face due to the welding processes.

In the elastic range, it was found that variation of strain over the depth of the beam was nearly linear at the critical section, with the exception of greater absolute values at the lower flange than would be extrapolated from the other data. Dogbone specimen strain values were elevated equally at the top and bottom faces of the bottom flange, while haunch values were only elevated at the bottom extreme fiber.

Design Implications and Conclusions

The two retrofit techniques investigated in this program were chosen because they were believed to represent potentially effective and economical means to increase the plastic rotation capacity of existing pre-Northridge welded flange-bolted web moment connections. Typical pre-Northridge connections were retrofit with either a bottom flange dogbone or a welded bottom haunch. For each retrofit technique, an effort was made to minimize welding or design modifications at the beam's top flange, in order to minimize the need to remove portions of the floor slab.

The use of the bottom flange dogbone, by itself, did not provide an improvement in connection performance. These connections failed by fracture of the existing E70T-4 beam flange groove welds at low levels of plastic rotation, comparable to that of an unretrofitted connection. Consequently, the use of a bottom flange dogbone, without improvements or

modifications to the beam flange groove welds, is not recommended. To achieve an improvement in plastic rotation capacity, it was necessary to remove the existing low toughness E70T-4 weld metal at the top and bottom beam flange groove welds, and reweld the beam with a higher toughness electrode. When replacement of the weld metal was combined with the bottom flange dogbone in a composite specimen, plastic rotations of about 0.020 radian were achieved. These connections, however, still failed by fracture of the beam flange groove welds. After fracture of the welds, the strength of the connections deteriorated rapidly.

The bottom flange dogbone was initially considered in this project as a simple and inexpensive retrofit measure. The need to replace the existing beam flange groove welds at both top and bottom flanges will likely significantly increase the cost of this option. Consequently, even though this approach permitted the development of 0.02 radian of plastic rotation, the bottom flange dogbone combined with weld replacement does not appear to be the most attractive retrofit option from the point of view of structural performance and economy.

For new construction applications, the dogbone connection has shown outstanding performance in laboratory testing. Dogbone connections for new construction differ significantly from the dogbone retrofit details tested here. Typical details for new construction include the use of dogbone cutouts in both the top and bottom flanges (the retrofit used only a bottom flange dogbone), the use of a welded web connection (the retrofit used a bolted web), and the use of continuity plates in the columns (the retrofit used no continuity plates). The use of some/all of these new construction details in a retrofit would likely improve the performance of the retrofitted connection from that observed in this program, but it would also add cost.

The welded bottom haunch specimens tested generally showed better performance than the dogbone specimens. In the welded haunch specimens, no modifications were made to the existing beam flange groove welds. Three of the four bare steel haunch specimens failed by fracture at the existing E70T-4 top flange welds at plastic rotations ranging from 0.012 to 0.023 radian. However, after fracture of an existing beam flange weld, the rate of strength deterioration of the haunch specimens was significantly less than that for the dogbone specimens. Even after fracture of the top flange weld, the haunch remains attached to the column and the bottom beam flange, providing substantial reserve strength and safety. Consequently, an advantage of the haunch is that it provides a degree of redundancy to the connection not available with the dogbone retrofit.

With the addition of a composite slab, the haunch specimens showed outstanding performance. Of the four composite haunch connections tested in this program, none experienced a fracture at the existing beam flange groove welds. Rather, the strength of these specimens deteriorated gradually due to local and lateral buckling of the beams without failure of the connection. These connections all developed in excess of 0.030 radian of plastic rotation without connection failure. At total plastic rotations of 0.020 radian, beam moments exceeded 80% of the peak values achieved in the tests. The composite specimens retrofitted with a bottom haunch, therefore, showed performance comparable to new construction standards, even though the existing low toughness E70T-4 beam flange groove welds were left in place. Similar performance was observed in bottom haunch retrofit tests by Uang et al. (1998). Consequently, when a composite floor slab is present, the use of a welded bottom haunch appears to provide significantly better structural performance than the dogbone retrofits tested in this program.

Several observations were made on the influence of a composite slab on the performance of the retrofitted connections.

The slab significantly reduced the severity of local and lateral buckling of the beam. This had two beneficial effects. First, the rate of strength degradation due to beam buckling was reduced. Further, the reduced severity of beam top flange buckling appeared to reduce strain demands at the top beam flange groove weld. It is believed that the reduction in the severity of top flange buckling was important in preventing top flange weld fracture in the composite haunch specimens.

The composite slab increased the strength of the connections by 10–30%. Past researchers have estimated the strength of moment connections for composite beams by using plastic analysis of the composite cross section. In these analyses, the effective width of the slab has generally been taken equal to the width of the column flange, and the effective concrete stress has been taken in the range of $1.3-1.8f'_c$. Data collected in this test program suggest that the effective width of the concrete depends both on the column flange width and on the column depth. Further, effective concrete stresses appeared to be substantially less than $1.3f'_c$ when subjected to reversed cyclic loading. These lower effective concrete stresses may have been due to the failure of welded shear studs in the specimens. The shear studs were fillet welded to the beams in this program, and many of these welds fractured in the course of testing. Overall, the results of these tests suggest further research is needed to accurately predict the strength of moment connections for composite beams as well as to predict the strength of shear studs under cyclic load.

ACKNOWLEDGMENTS

Primary sponsorship of this research was provided by a grant from the National Institute of Standards and Technology (NIST Award No. 70NANB5H0128). The research was cosponsored by the Northridge Steel Industry Research Fund. This fund's contributors and participants are the American Institute of Steel Construction, the Structural Shape Producers Council, the American Iron and Steel Institute, the California Field Ironworkers Trust, the Steel Service Center Institute, the Steel Joist Institute, and the Lincoln Electric Foundation. In addition, the Structural Shape Producers Council donated the structural steel used for the construction of test specimens. The writers gratefully acknowledge the support of these organizations. The writers would also like to thank the following individuals for assistance and suggestions provided on this research project: Prof. Kazuhiko Kasai of the Tokyo Institute of Technology, Prof. Chiaming Uang of the University of California at San Diego, Nestor Iwankiw of AISC, James O. Malley of Degenkolb Engineers, and Duane Miller of Lincoln Electric.

APPENDIX. REFERENCES

- AISC manual of steel construction load and resistance factor design. (1994). 2nd Ed., American Institute of Steel Construction, Chicago.
- ATC-24: guidelines for seismic testing of components of steel structures. (1992). Applied Technology Council, Redwood, Calif.
- AWS D1.1-9: structural welding code—steel. (1996). American Welding Society, Miami.
- Chen, S. J., Yeh, C. H., and Chu, J. M. (1996). "Ductile steel beam-to-column connections for seismic resistance." *J. Struct. Engrg.*, ASCE, 122(11), 1292–1299.
- Civjan, S. A. (1998). "Investigation of retrofit techniques for seismic resistant steel moment connections," PhD dissertation, The University of Texas at Austin, Austin, Tex.
- Du Plessis, D. P., and Daniels, J. H. (1972). "Strength of composite beam to column connections." *Rep. No. 374.3*, Fritz Engrg. Lab., Lehigh University, Bethlehem, Pa.
- Engelhardt, M. D., and Husain, A. S. (1993). "Cyclic-loading performance of welded flange-bolted web connections." *J. Struct. Engrg.*, ASCE, 119(12), 3537–3550.
- Engelhardt, M. D., and Sabol, T. A. (1994). "Testing of welded steel moment connections in response to the Northridge earthquake." *Progress Rep. to AISC Advisory Subcommittee on Special Moment Resisting Frame Res.*, University of Texas at Austin, Austin, Tex.
- Engelhardt, M. D., Winneberger, T., Zekany, A. J., and Potyraj, T. J. (1996). "The dogbone connection. II." *Modern Steel Constr.*, August, 46–55.
- Federal Emergency Management Agency (FEMA). (1995). "Interim guidelines: evaluation, repair, modification and design of steel moment frames." *FEMA-267 (SAC-95-02)*, Washington, D.C.
- Federal Emergency Management Agency (FEMA). (1997a). "Connection test summaries." *FEMA-289*, Washington, D.C.
- Federal Emergency Management Agency (FEMA). (1997b). "Interim guidelines advisory no. 1." *FEMA-267A (SAC-96-03)*, Washington, D.C.
- Gross, J. L., Engelhardt, M. D., Uang, C. M., Kasai, K., and Iwankiw, N. R. (1999). "Modification of existing welded steel moment frame connections for seismic resistance." *Steel Des. Guide Series No. 12*, American Institute of Steel Construction, Chicago.
- Iwankiw, N. R., and Carter, C. J. (1996). "The dogbone: a new idea to chew on." *Modern Steel Constr.*, April, 18–23.
- Kaufmann, E. J., Fisher, J. W., Di Julio, R. M., and Gross, J. L. (1997). "Failure analysis of welded steel moment frames damaged in the Northridge earthquake." *Rep. NISTIR 5944*, National Institute of Standards and Technology, Gaithersburg, Md.
- Lee, S. J., and Lu, L. W. (1989). "Cyclic tests of full-scale composite joint subassemblies." *J. Struct. Engrg.*, ASCE, 115(8), 1977–1998.
- Leon, R. T., Hajjar, J. F., and Gustafson, M. A. (1998). "Seismic response of composite moment-resisting connections: I: Performance." *J. Struct. Engrg.*, ASCE, 124(8), 868–876.
- Miller, D. K. (1996). "Lessons learned from the Northridge earthquake." *Welding in the World/Le Soudage dans le Monde*, Amsterdam, 38(November), 257–276.
- Ojdrovic, R. P., and Zarghamee, M. S. (1997). "Fracture of steel moment connections in the Northridge earthquake." *Proc., Inst. of Civ. Engrs., Struct. and Build.*, London, 122(2), 209–217.
- Plumier, A. (1995). *Summary of technical data on beams using reduced sections as dissipative zones*. University of Liege-Belgium, Liege, Belgium.
- Popov, E. P., Amin, N. R., Louie, J. J. C., and Stephen, R. M. (1986). "Cyclic behavior of large beam-column assemblies." *Engrg. J., Am. Inst. of Steel Constr.*, 23(1), 9–23.
- Proc., AISC Special Task Committee on the Northridge Earthquake Meeting. (1994). American Institute of Steel Construction, Chicago.
- Sabol, T. A., and Engelhardt, M. D. (1996). *Welded steel moment frame joint testing programs*. Engelkirk & Sabol, Inc., Los Angeles.
- Shuey, B., and Engelhardt, M. D. (1996). "Testing of repair concepts for damaged steel moment connections." *Tech. Rep. on Exper. Investigations of Beam-Column Subassemblies; Rep. No. SAC 96-01*, SAC, Sacramento, Calif.
- Tagawa, Y., Kato, B., and Aoki, H. (1989). "Behavior of composite beams in steel frame under hysteretic loading." *J. Struct. Engrg.*, ASCE, 115(8), 2029–2045.
- Tremblay, R., Tchebotarev, N., and Filiatrault, A. (1997). "Seismic performance of RBS connections for steel moment resisting frames: influence of loading rate and floor slab." *Proc., STESSA 1997*, Kyoto, Japan, 4–7.
- Tsai, K. C., Wu, S., and Popov, E. P. (1995). "Experimental performance of seismic steel beam-column moment joints." *J. Struct. Engrg.*, ASCE, 121(6), 925–931.
- Uang, C. M., and Bondad, D. (1996). "Static cyclic testing of pre-Northridge and haunch repaired steel moment connections." *Rep. No. SSRP-96/02*, SAC, Sacramento, Calif.
- Uang, C. M., and Noel, S. (1995). *Brief summary on cyclic response of specimen COH-1*. University of California, San Diego.
- Uang, C. M., Yu, Q. S., and Noel, S. (1998). "Rehabilitating pre-Northridge steel moment frame connections: RBS and haunch approaches considering slab effects." *Proc., 6th U.S. Nat. Conf. on Earthquake Engrg.*, Earthquake Engineering Research Institute, Oakland, Calif.
- Xue, M., Kaufmann, E. J., Lu, L. W., and Fisher, J. W. (1997). "Fracture and ductility of welded moment connections under dynamic loading." *Building to Last: Proc., Struct. Congress XV*. ASCE, Reston, Va., 607–613.
- Yang, T. S., and Popov, E. P. (1995). "Behavior of pre-Northridge moment resisting steel connections." *Rep. No. UCB/EERC-95/08*, Earthquake Engrg. Res. Ctr., University of California at Berkeley, Berkeley, Calif.
- Youssef, N. F. G., Bonowitz, D., and Gross, J. L. (1995). "A survey of steel moment-resisting frame buildings affected by the 1994 Northridge earthquake." *Rep. NISTR 5625*, National Institute of Standards and Technology, Gaithersburg, Md.